




Enhancement of Power Quality in an Actual Hot Rolling Mill Plant Through a STATCOM

Gonzalo Arturo Alonso Orcajo , *Member, IEEE*, Josué Rodríguez Diez , José M. Cano , *Member, IEEE*, Joaquín G. Normiella, Joaquín Francisco Pedrayes González, Carlos H. Rojas, Pablo Ardura G, and Diego Cifrián R

Abstract—A strategic use of a static synchronous compensator (STATCOM) for providing dynamic reactive power management of a hot rolling mill plant along with active mitigation of harmonics is considered in this article. More specifically, the behavior of a cascaded H-bridge (CHB) converter-based STATCOM is assessed. The impact of the steel to be milled and the specific features of the plant on the design of the STATCOM is discussed. The proposed strategy is analyzed from the point of view of reactive power flow management, active power loss reduction, and voltage control at the coupling point, as well as harmonics reduction and decrease of unscheduled shutdowns in the event of a trip in the passive filtering system. The article is based on real plant measurements, simulation tests, and results from an experimental platform built at scale, and represents the first stage of an ambitious plan to renew this type of plants aimed at transforming them into active elements for electrical energy management.

Index Terms—Cascaded H-bridge converter (CHB), filtering banks, finishing mill, hot rolling mill, power system harmonics, roughing mill, static synchronous compensator (STATCOM), steel.

I. INTRODUCTION

STEEL industry is considered to be an energy-intensive industry [1]. Efficient use of energy plays a strategic role in steel industry, which is the industrial sector with the highest energy demand in numerous countries. Energy consumption accounts for between 15% and 20% of the operating costs of a steel plant and has direct implications on other costs, e.g., those associated with the emission of greenhouse gases (GHG). More

specifically, hot rolling mills are responsible for approximately 8% of the total energy demand in integrated steel industries and also for the highest electric power demand in steel plants without arc furnaces.

The average electric energy consumption in the hot rolling operation is between 70 and 80 kWh per ton of steel coil produced. Power quality is also of great importance because steel plants, as large consumers, have a powerful capacity to affect the distribution network and are particularly sensitive to possible disturbances. Rolling mill campaigns handle 20–30 slabs per hour and approximately 470–530 slabs per day. Each slab can weigh up to 22–26 tons; therefore, the daily demand in steel plants can reach up to 1 GWh, which is why proposals aimed at improving the energy efficiency of this industrial activity offer a great opportunity for considerable energy savings [1].

This article seeks to develop a procedure to improve a great number of hot rolling mill plants based on classic topologies, which are predominant in facilities launched in the 90 s and currently still in service. These facilities are constituted by rolling stands comprising cycloconverters of 12 or more pulses and passive filtering systems for compensating reactive power and canceling harmonics [2]–[4]. To improve the efficiency and productivity of this type of plants, a strategic use of a static synchronous compensator (STATCOM) is considered [5], [6]. Multilevel voltage-source converter (VSC) configurations are the most popular in MV STATCOMs for high-power applications [7]. Among such configurations, neutral-point clamped (NPC), flying capacitor, and cascaded H-bridge (CHB) converter have been widely used in power systems to control the reactive power flow and improve the preeminent power quality indexes. CHB-based STATCOMs provide notable flexibility, remarkable dynamics, a significant difference between ac-side and dc-side voltages, simple scalability, and a high value of the switching frequency associated with the output waveform with respect to that of the bridge converters, thus enabling a thorough current control [8]–[10].

An actual plant located in South America with a topology similar to that in other hot rolling mill plants currently operating in different countries is considered (Fig. 1). An intensive measurement campaign is conducted under different rolling conditions. Various problems are detected regarding power quality and the reliability of the system against failures under the original operating conditions. The solution proposed to solve these problems consists in connecting a STATCOM to the point of common coupling of the rolling stands. The objectives in sizing

Manuscript received June 28, 2019; revised October 29, 2019 and February 2, 2020; accepted February 13, 2020. Date of publication February 24, 2020; date of current version April 24, 2020. Paper 2019-METC-0685, presented at the 2019 IEEE Industry Applications Society Annual Meeting, Baltimore, MD, USA, Sep. 29–Oct. 3, and approved for publication in the IEEE TRANSACTIONS ON INDUSTRY APPLICATIONS by the Metals Committee of the IEEE Industry Applications Society. This work was supported in part by the Research and Development Center of ArcelorMittal (Spain) and in part by the Ministry of Economy and Competitiveness of Spain (projects within the framework of the National Plan of Research, Development, and Innovation, reference DPI2017-89186-R). (*Corresponding author: Gonzalo Arturo Alonso Orcajo.*)

Gonzalo Arturo Alonso Orcajo, José M. Cano, Joaquín G. Normiella, Joaquín Francisco Pedrayes González, and Carlos H. Rojas are with the Electrical Engineering Department, University of Oviedo 33204 Gijón, Spain (e-mail: gonzalo@uniovi.es; jmcano@uniovi.es; jgnormiella@uniovi.es; pedrayesjoaquin@uniovi.es; chrojas@uniovi.es).

Josué Rodríguez Diez, Pablo Ardura G, and Diego Cifrián R are with the Basque Country Research Centre of ArcelorMittal, Sestao and the Global Research and Development Department 33400 Avilés, Spain (e-mail: josue.rodriguezdiez@arcelormittal.com; pablo.ardura@arcelormittal.com; diego.cifrian@arcelormittal.com).

Color versions of one or more of the figures in this article are available online at <http://ieeexplore.ieee.org>.

Digital Object Identifier 10.1109/TIA.2020.2976034

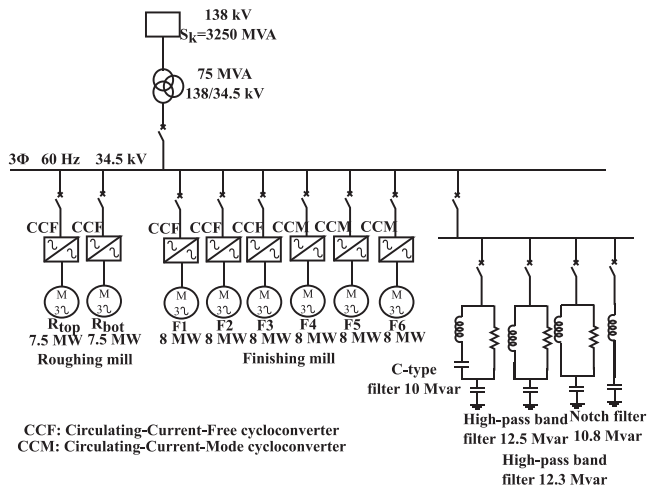


Fig. 1. Single-line diagram of the original plant.

and designing the STATCOM must be set in coordination with the passive filtering system and are as follows: 1) reduction of the rms value of the current upstream the point of common coupling (PCC); 2) reduction of the voltage drop in the PCC to comply with the existing standards; 3) improvement of the global power factor (PF) of the plant; 4) adaptation of the harmonic distortion rate to the requirements set by the existing regulations; 5) support in case of accidental disconnection of the filtering branches; 6) inhibition of possible resonances; and 7) improvement of the plant immunity against voltage sags.

The drives included in the rolling mill plants are constantly evolving. The improvement measurements are expected to be integrated progressively to provide added value to the plant and to be compatible over time with the global renewal of rolling stands [11]–[13]. The incorporation of a STATCOM is an option compatible with other future enhancements of the plant including those regarding a renewal of the rolling stands to adapt to new technological advances. The design of the converter is conducted in the light of the real operating conditions of a hot rolling mill plant.

The improvement proposal foresees the adaptation of the production and power systems in the coming years and is part of an ambitious plan aimed at transforming progressively the rolling mill into an active element for the management of electrical energy. The new equipment must be compatible with the normal operation of the original plant and maintain this compatibility once the renewal is completed. The improvement process consists of the following stages: 1) incorporation of a STATCOM compatible with the original cycloconverters and the passive filtering system; 2) progressive replacement of the conventional cycloconverter-based rolling stands by others based instead on back-to-back converters with active front end (AFE) rectifiers capable of exercising individual control over the flow of active and reactive power and the injection of harmonics; 3) elimination of passive filtering branches; and 4) coordinated management of the reactive power flow values. In short, the final target is aimed at offering solutions for the increasingly high demand of efficiency and active management of energy in energy-intensive industries.

TABLE I
CHEMICAL COMPOSITION OF THE THREE TYPES OF STEEL

Element	Steel A - Content (%)	Steel B - Content (%)	Steel C-Content (%)
Manganese	≤ 0.6	≤ 1.2	≤ 1.35
Carbon	≤ 0.12	≤ 0.22	≤ 0.25
Sulfur	≤ 0.045	≤ 0.035	≤ 0.04
Phosphorous	≤ 0.045	≤ 0.035	≤ 0.035

II. ACTIVE AND REACTIVE POWER DEMAND

The hot rolling mill under consideration comprises one roughing mill (RM) and six finishing mill (FM) stands. RM consists of two stands: one at the top side and the other one at the bottom. FM consists of six stands. Only three stands (F4, F5, and F6, see Fig. 1) are equipped with circulation-type, 12-pulse, three-phase cycloconverters [2]. These stands avoid the over-compensation at the PCC, upstream from the filtering system. The rest of the stands are circulating-current-free and double-cascade-connected cycloconverter drives. The rated values in the main equipment are shown in Fig. 1. The motors are synchronous and fed by field-oriented control (FOC) based cycloconverters. The plant is connected to a 138-kV voltage level through a 75-MVA, 138/34.5-kV transformer. The global passive filter enables the compensation of 45 Mvar at 34.5 kV.

Despite the fact that the article regards a specific plant and the measurements obtained in the actual plant are certainly available, the complete process for calculating the active and reactive power profiles and sizing the passive filtering system is described as follows in order to facilitate the analysis of other types of plants.

An in-depth analysis of the network active and reactive power profiles under different rolling conditions must be performed prior to the design of the compensation system. Three types of steel with different carbon content are considered to exemplify the analytical procedure conducted to obtain the active and reactive power demand profiles corresponding to each stand. The chemical composition of each type of steel and its mechanical properties can be obtained from the standard (Table I). Standard SAE J403 1010 [14] is used for type “A” steel, NBR 6655 LN280 [15] for type “B,” and ASTM A1011 SS36 [16] for type “C.”

The roughing mill provides the steel with the correct thickness to enter the finishing mill train. In the three analyzed cases, five passes are run in the roughing stand. The steel plate leaving the roughing mill is subjected to a single pass in the continuous finishing train, where the required final dimensions are achieved. The analytical procedure for obtaining the load profiles of each of the rolling cylinders as well as the active and reactive power profiles has been described in detail in previous work [17], [18]. Simulation programs to predict the properties of hot strip steels from the rolling conditions, e.g., *Stripcam* or *HSMM*, must be used. These programs are capable of correlating the rolling process variables with the steel mechanical properties to be obtained. The strip thickness at the delivery side of each stand has been chosen (Fig. 2) by considering the constraints in power and speed (Fig. 3). The demanded active power is directly calculated from the values of the torque, speed of the motors, and performance ratio of the system. Reactive power values

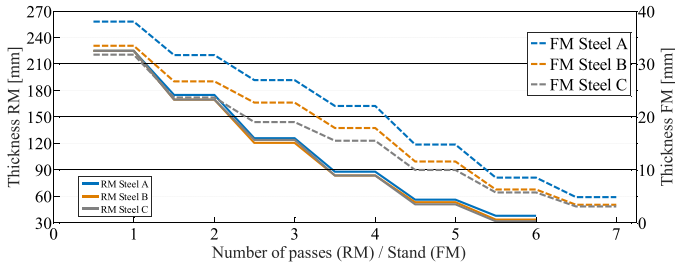


Fig. 2. Thickness [mm] of the slab calculated in roughing and finishing mills.

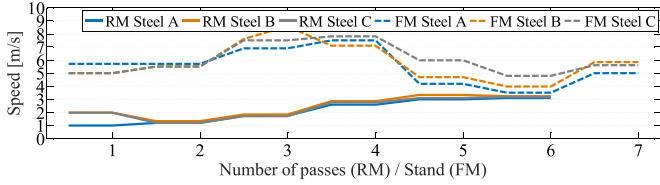


Fig. 3. Speed reference calculated in roughing and finishing mill.

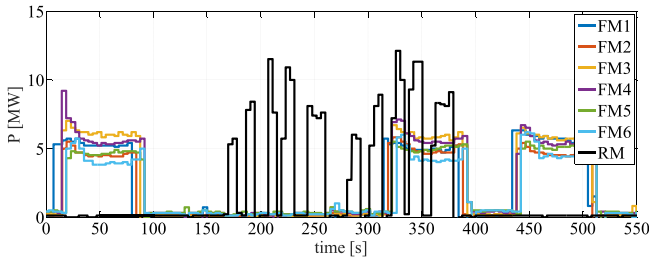


Fig. 4. Actual active power profile of the roughing and finishing mill stands.

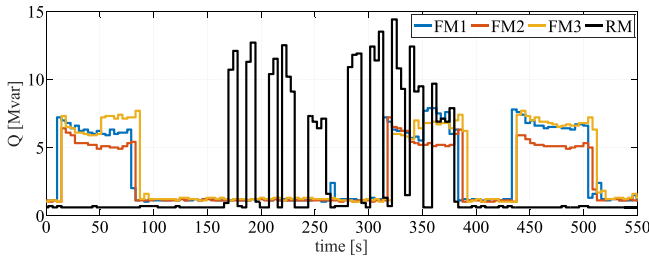


Fig. 5. Actual reactive power profile of the roughing and finishing mill stands.

are obtained from the cycloconverter mean trigger angle and the active power profile. Power flow evolutions during a rolling campaign of the slabs in the actual plant are shown in Figs. 4 and 5. These measurements enable the contrast of the results. Global and actual values corresponding to the three analyzed slabs are shown in Fig. 6.

The profiles are referred to the first 550 s of a rolling campaign in the actual plant when 11 different slabs are rolled and active and reactive power values are recorded. Hereinafter, this profile of about 38 min is referred to as “benchmark profile.”

III. PASSIVE FILTER DESIGN

Once the active and reactive power demands have been calculated, the second step consists in analyzing the passive filtering

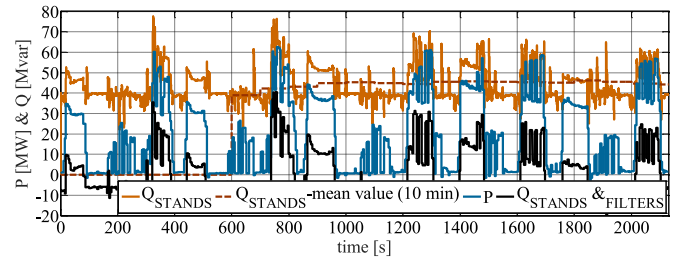


Fig. 6. Active and reactive power demands of the hot rolling mill.

system. Although the plant under study maintains its original passive filtering bank, the criteria used for its sizing are reviewed in order to understand the role played by the STATCOM and its most proper design requirements. To determine the rated power of the passive filtering system, the reactive power of the load and the injection of harmonics in the network are analyzed during normal operation before the filter has been connected, which corresponds to the profile described in the previous section (see red line in Fig. 6). The average value obtained is 45 Mvar, which determines the rated power of the filtering bank.

Given that the original drives consist of 12-pulse, three-phase cycloconverters, the spectrum of the supply currents contains a series of sideband harmonics dependent on the grid frequency, f_i , and the output frequency of the cycloconverter, f_o , which, in turn, depends on the motor speed and the number of pole pairs. Although the finishing and roughing mill drives have a 12-pulse topology, significant harmonics of orders 5 and 7 are found in the actual spectra due to the presence of asymmetries in the operation of the drives and tolerances in the transformer windings [19]. To comply with the standard limitations and the compensation of reactive power, a passive filtering system consisting of four banks is defined [20], [21]. To reduce the impact of the fifth and seventh harmonics, two filtering banks are selected, one of them being a notch filter tuned for a frequency of order 4.08, and the other one being a high-pass filter for a frequency of order 6. Harmonics of orders 11, 13, and higher are damped by a high-pass filter tuned to a frequency of order 10. Moreover, a C-type filter playing the role of a capacitive damped network works along with the three aforementioned filters to compensate jointly for the reactive power. The evolution of the reactive power values under the same rolling conditions upstream the PCC and after the filter connection is shown in Fig. 6.

IV. STATCOM TOPOLOGY

A cascaded H-bridge converter is selected as the most suitable alternative for the present application (Fig. 7). As already described in Section I, this topology provides important advantages over its competitors. Its modular configuration offers the possibility of handling high power with high switching frequencies in MV grids. Furthermore, it has interesting features from the point of view of power quality. In this article, a 34.5-kV, 15-MVA wye-connected STATCOM is considered. It includes 22 cascaded H-bridge pulse width modulation (PWM) converters per phase, which leads to a 45-level waveform in phase

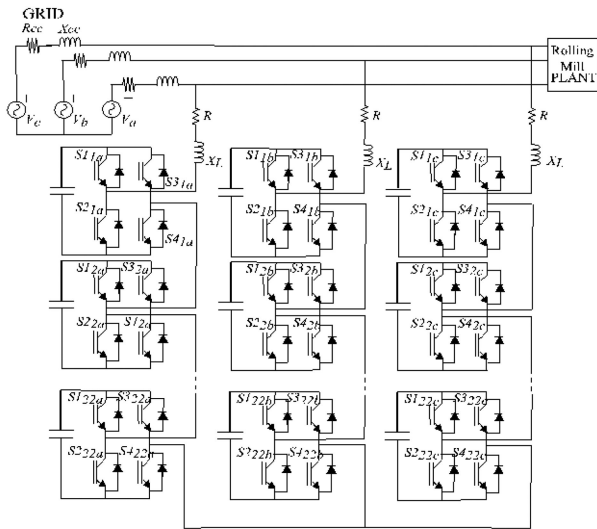


Fig. 7. CHB STATCOM topology.

TABLE II
PARAMETERS OF THE STATCOM

Grid Voltage	34.5 kV	DC capacitor	1800 μ F
Rated Power	15 MVA	DC capacitor voltage	1600 V
AC inductor-stray resist.	0.793 Ω	Number of H-bridges	22
AC inductor-inductance	10.7 mH	PWM carrier freq.	300 Hz

voltage. Thus, a total number of 66 H-bridge cells are used in the final design. Each cell is equipped with a film capacitor rated at 1800 μ F, and controlled to follow a reference voltage of 1600 V. The STATCOM is directly coupled to the grid through an ac inductor, avoiding the use of a transformer. Table II shows the specific values of the main characteristics and components of the device. Phase-shifted PWM (PS-PWM) was selected as the modulation technique to be used in this application [13]. All cells are modulated using the same reference signal with a carrier frequency of 300 Hz.

To determine the size of the STATCOM, a scenario involving highly demanding rolling conditions is considered. The selected scenario is sufficiently representative of both the power demand (active and reactive) and the harmonic distortion (Fig. 6), thus enabling the detection of possible deficits of the system when attempting to satisfy that demand. The economic impact of the proposed approach is also studied. The cost analysis must consider the STATCOM size, the power losses, the deviation of the system with respect to its setpoint value, both the voltage and the reactive power at the nodes, and unforeseen production stoppages.

The future retrofit of the rolling stand drives affects the reactive power demand, thus the STATCOM being sized at this stage according to the minimum rated power required to overcome the most unfavorable circumstances. Therefore, the size of the STATCOM was selected based on the following two main objectives.

- 1) It must serve as a backup for the passive filtering system. In fact, this is one of the main motivations to add

the STATCOM to the installation. This task imposes a minimum rated power for the equipment of 12.5 Mvar, which is the highest-rated power of the four branches of the passive filter bank under analysis. In the event of tripping of the protections of one of these branches, the STATCOM can temporarily assume its reactive power contribution at the expense of neglecting other less critical power quality features during the emergency contingency.

- 2) The STATCOM is in charge of avoiding exceeding the limits of maximum rapid voltage changes imposed by the standards [22], [23] under normal operating conditions. For the analyzed operating conditions, simulations show that the minimum size that avoids reaching these limits is 15 MVA. Certainly, reducing this size just to 14.5 MVA leads to not complying the regulations due to a number of events per hour, showing rapid voltage changes greater than 4%, higher than the one imposed by the standard. In Section V-B, the influence of the STATCOM rated power on the voltage variations is analyzed in detail.

Rolling mill plant including a 15-MVA STATCOM is simulated by using general-purpose software for analyzing electrical power systems [24]. The simulations enable the verification of the fulfillment of the objectives pursued with the incorporation of a STATCOM. All simulation results are based on a 45-level cascaded H-Bridge STATCOM. All elements of the global system are simulated simultaneously, i.e., rolling mill plant and the STATCOM along with its control system. Balanced conditions have been considered.

A. Power Modules

The design of the converter is based on IGBT technology [25], with power modules with a dynamic blocking voltage of 3300 V and maximum phase current of 600 A. The rated current of the IGBT modules is selected according to the maximum current expected during the specific operating conditions of the hot rolling mill. Taking into account the rated power of the STATCOM, 15 MVA, and grid voltage, which can be considered within acceptable limits until 0.9 pu. of its rated value, 34.5 kV, the expected maximum current reaches 395 A. In addition, a 1.4 oversizing factor is considered in the design to be aware of transient overloads, which raises the minimum current of the power modules to 553 A. Thus, IGBT power modules rated at 600 A are selected, which fully complies with the design requirements.

The dynamic blocking voltage of the selected IGBT power module is 3300 V, which is acceptable for an expected dc capacitor voltage value, V_{dc} , of 1600 V. This capacitor voltage value is selected to assure a modulation index, m , near 0.8, and can be immediately derived from the number of converter modules per phase, 22, (see next section) and the resulting output voltage of 905 V per module needed to comply with the grid rated voltage, 34.5 kV.

B. Number of H-Bridge Cells

The number of H-bridge cells per leg, n , must be determined according to the rated voltage of the STATCOM and the blocking

voltage of the selected IGBT power modules [26]. The selection of a dc capacitor voltage, V_{dc} , around half the value of the blocking voltage of the power modules is a common practice in converter design. Setting this value to 1600 V and considering a modulation index, m , of 0.8, as an acceptable rate at normal operating conditions, leads to an ac rms cell output voltage of 905 V. Thus, the number of cascaded voltage-source H-bridge cells per phase, n , can be obtained as

$$n = \frac{v_{\text{phase}}}{v_{\text{converter}}} = \frac{34500}{\frac{\sqrt{3}}{905}} = 22 \text{ cells per phase.} \quad (1)$$

The selection of 22 H-bridge cells per phase results in a 45-level converter. Thus, if phase-shifted PWM is considered, the carrier frequency of each cell, f_c , can be as low as 300 Hz. In that case, the phase voltage seen from the STATCOM terminals is equivalent to a carrier signal of 13.2 kHz [8].

D. Capacitors

The film capacitors used in the converter design must comply with a set of self-evident requirements, such as low power dissipation, rated voltage compatible with utilization values, and reduced size consistent with the space constraints or low cost. The selection of the capacitance value must be determined according to the maximum dc voltage ripple, ΔV_C , compatible with a proper performance [27]. Thus, a 1.8-mF capacitor was selected that fully complies with the stated requirements.

E. Coupling Inductance

The coupling inductance of the converter, L_s , is designed according to the constraints of the STATCOM system. A minimum value of this inductance is imposed by the maximum acceptable ripple of the output current, Δi_C , taking into account the selected number of H-bridge cells in each leg, n , the selected switching frequency, f_c , and dc-link voltage value, V_{dc} , [28], [29]. The upper limit for the coupling inductance value is determined by the possibility of delivering the full reactive power of the STATCOM at rated conditions. An inductor of 10.7 mH was used in the final setup, which fully complies with the aforementioned requirements.

The control system of the cascaded H-bridge STATCOM comprises four control loops (see Fig. 9).

- 1) *DC voltage regulator*: An outer loop that corresponds to the dc voltage control. It is used to control the dc voltage of the cell capacitors.
- 2) *AC voltage regulator*: An outer loop that corresponds to the ac voltage control. It is used to control the rms value of the ac voltage at the point of common coupling. Reference i_{q^*} for the q -axis loop is obtained by summing the ac-voltage regulator output and the q -axis component of the reactive power regulators at the fundamental frequency. The ac voltage regulator generates a fraction of the q -axis current reference that must be added to the reference obtained to compensate for the reactive power demand at the fundamental frequency.
- 3) *Current regulator*: An inner loop that regulates the STATCOM currents to compensate for the demand of reactive

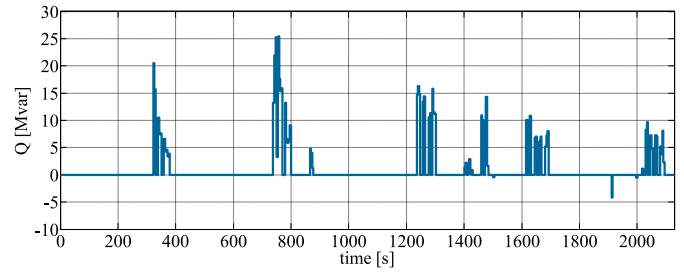


Fig. 8. Reactive power surplus upstream the PCC.

power at the fundamental frequency upstream the PCC, to mitigate the current harmonic distortion caused by the rolling mill drives, and to control the capacitor (dc) and grid (ac) voltages. It is based on a proportional-integral (PI) regulator, which sets the values of the current components in the synchronous reference frame, i_d and i_q . The system responsible for the cancellation of harmonics is based on multiple rotating integrators (MRI), and has been previously used with success in this type of applications by other authors [30]–[33]. This control technique has a clear advantage over other alternatives due to its inherent modular structure, which allows to select freely those specific harmonics allocated for compensation (in this case, harmonics of order 5, 7, 11, and 13 as well as those corresponding to the resonant conditions coming from the passive filter bank). The cancellation is performed in the dq reference frame through the use of MRI based on pure integrators.

- 4) *Capacitor voltage balancing regulator*: This task is accomplished through two stages, as proposed in [34]–[36].
 - 1) An interphase dc-link voltage balancing scheme is in charge of guaranteeing that the sum of the capacitor voltages of each phase is made equal to the reference value.
 - 2) An individual voltage balancing control is devoted to assure that the capacitor voltage of each H-bridge unit is made equal to the reference value.

V. ROLE PLAYED BY STATCOM

Despite the important role played by the passive filtering system, the integration of a STATCOM enables the cancellation of the dynamic variations of the reactive power remnants, the performance of a tight control of the voltage at the PCC, the reduction of losses in service, and the operation of the plant even if one of the branches of the passive filtering system is out of service, thus preventing the economic losses entailed in an operator being forced to stop the process [19].

A. Objective 1: Reducing Residual Reactive Power Flow

The proposed solution, based on the use of a 15-MVA STATCOM, is capable of reducing the global flows of reactive power, although they are not totally cancelled. Therefore, surpluses of reactive power (see Fig. 8) are responsible for the existence of additional losses, which are not high due to the low equivalent resistance of the transformer. The connection of the STATCOM

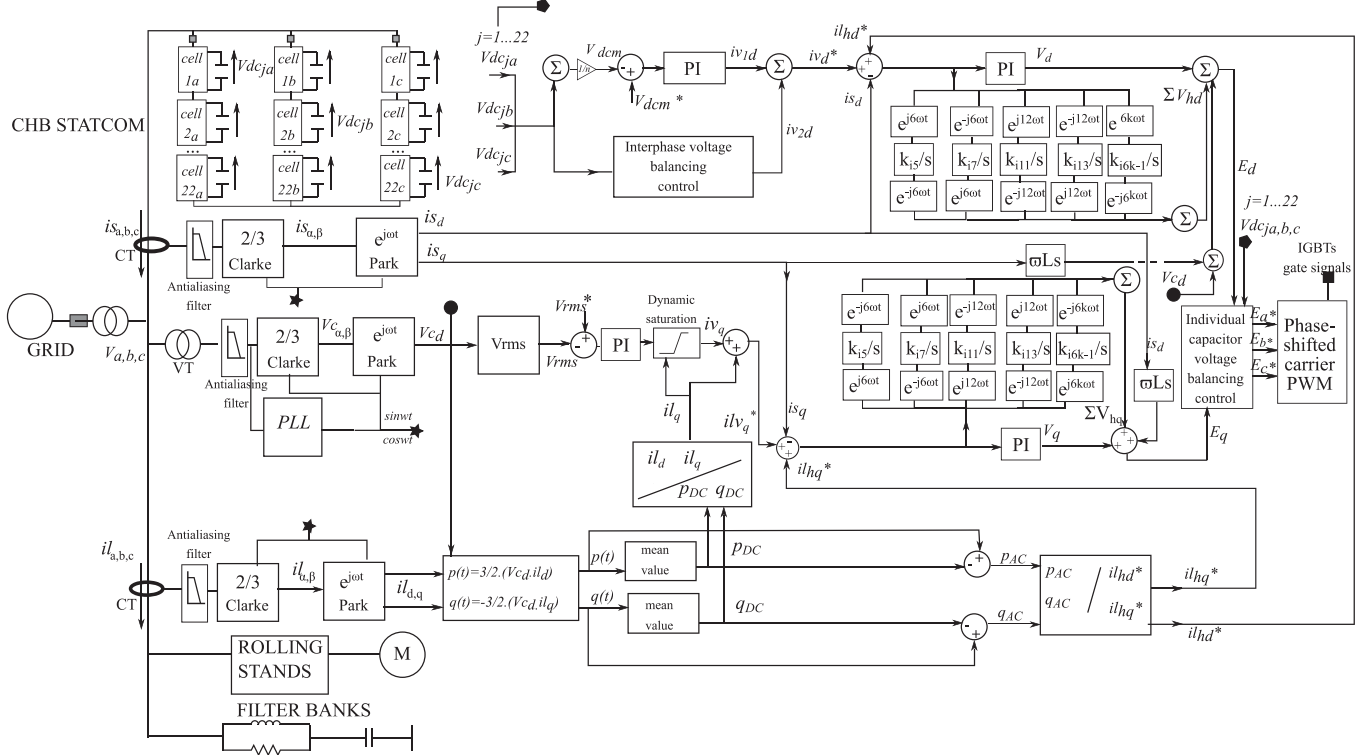


Fig. 9. Scheme of the control systems of the H-bridge STATCOM.

saves around 10 kWh of energy losses just in the transformer over the considered time interval.

Despite the effort made to cancel the reactive power, the high active power flow continues to determine the high current rms value and the losses in the distribution transformer.

The total losses of the STATCOM are related to the switching losses, the average power dissipated during the ON-state of the semiconductor switches in the modular converters, the capacitor losses, and the winding and core inductor losses. The semiconductor losses in the MMC can be potentially reduced to less than 1% [27]. The energy losses estimated by using the simulation model are approximately 0.78% of the energy brought into play by the STATCOM.

B. Objective 2: Limiting Voltage Variations

The voltage drop upstream the PCC depends on the active and reactive power flow in the said distribution network as well as on the value of its short-circuit impedance. According to CEI-61000-3-7: 2008 [22] and IEEE Std 1453.1-2012 [23], under normal operating conditions, in the connection of fluctuating loads to MV networks, voltage variations are limited to 3% of the rated value. However, these levels can be occasionally exceeded. The planning levels for rapid voltage variations are shown in Table III. As can be seen in Fig. 10, without the participation of the filtering banks, all these limits are exceeded. Moreover, even with the integration of the passive filtering system, it is not possible to comply with the planning levels provided by the standard. The integration of a 15-MVA STATCOM, with voltage

TABLE III
PLANNING LEVELS FOR RAPID VOLTAGE CHANGES AS A FUNCTION OF THE NUMBER OF CHANGES IN A GIVEN PERIOD [24]

Number of changes, n	$\Delta U/U_N$ %	
	MV	HV/EHV
$n \leq 4$ per day	5-6	3-5
$n \leq 2$ per hour, > 4 per day	4	3
$2 < n \leq 10$ per hour	3	2.5

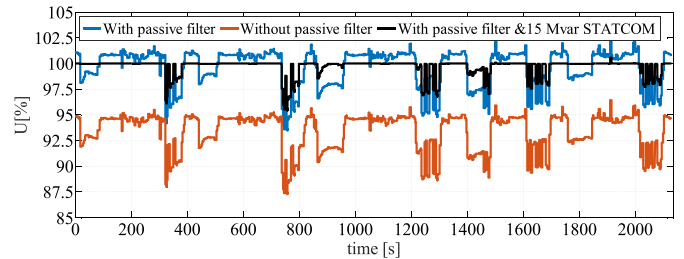


Fig. 10. Rapid voltage variations taking place during a critical rolling campaign.

control, restricts rapid voltage variations to 4.5%. The maximum variations arise during the peak demand of active power in the rolling process of the hardest steels. The STATCOM cancels the reactive power demand from the plant and supplies an extra of reactive power to compensate for the voltage drop caused by the delivery of active power. Along the benchmark profile shown in Fig. 6, 11 slabs get through the rolling process, resulting in an average production of 22 slabs per hour. Thus, the PCC would

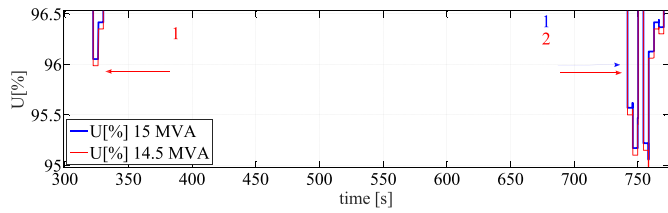


Fig. 11. Detailed view of the greatest rapid voltage variations taking place during the first half of an hour of a critical rolling campaign.

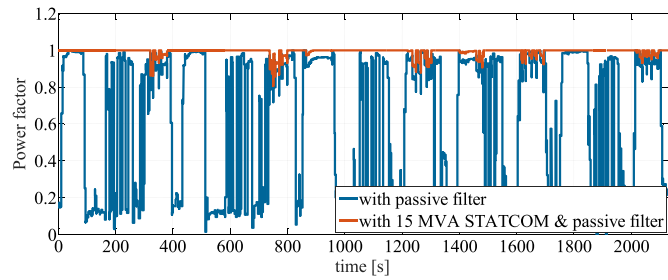


Fig. 12. Power factor at the PCC.

experience four rapid voltage variations greater than 3% and two greater than 4% per hour, which turn to be compatible with the planning levels shown in Table III. Certainly, reducing this size just to 14.5 MVA leads to not complying the regulations due to a number of events per hour, showing rapid voltage changes greater than 4%, higher than the one imposed by the standard. In order to illustrate this fact, Fig. 11 highlights an event that violates the rapid voltage variation limit of 4% only when the size of the STATCOM is lower than 15 MVA. This event makes the 14.5 MVA version not valid, as it reaches the trigger level of four events per hour imposed by the standard.

C. Objective 3: Improving Power Factor

In Fig. 12, the evolution of the PF of the plant without STATCOM is seen. Low values of the PF arise, especially at instants with low active power demand.

Additionally, the figure shows the expected PF of the plant after the installation of a 15-MVA STATCOM with voltage control. In these improved conditions, the PF remains greater than 0.98 most of the time. Industrial plants are normally subjected to penalties or bonus, as appropriate, according to their performance in terms of PF values. Moreover, complementary services of voltage control upstream of the PCC, carried out through the regulation of the reactive power flow from the plant, are optional and remunerated in several countries [37], [38].

D. Objective 4: Reducing Harmonic Distortion and Providing Support in the Event of Disconnection of Filter Banks

The STATCOM can reinforce the filtering action of the passive system by attenuating the most significant harmonics. It may also act as a redundant system that supports the action of the passive filters in the event that one of its branches is taken out of service. By using a control method based on MRI, the STATCOM injects

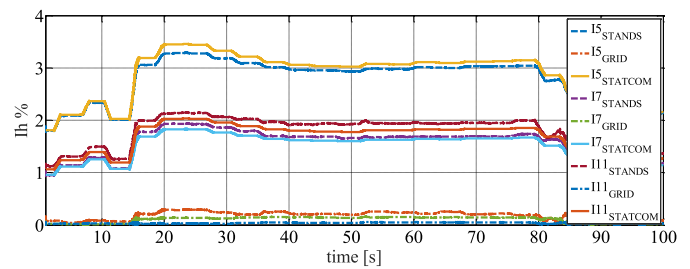


Fig. 13. rms value of the main current harmonics corresponding to the rolling stands, to the STATCOM, and to the grid upstream the PCC.

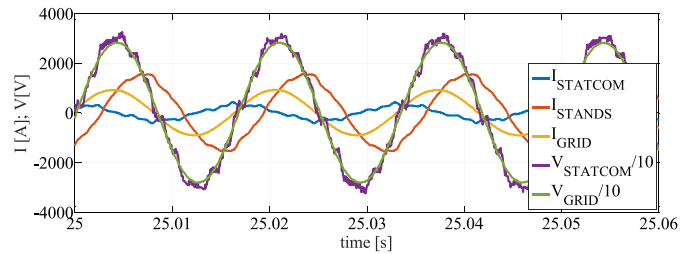


Fig. 14. Main variables involved in the active filtering action.

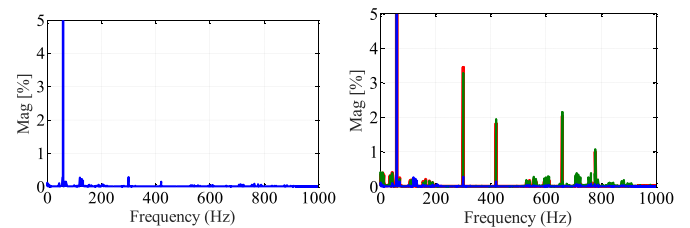


Fig. 15. *Left*: spectrum of the current circulating through the distribution network. *Right*: spectrum of the current flowing through the network (blue), STATCOM (green), and rolling stands (red).

selected harmonic currents into the system in phase opposition to those demanded by the roughing and finishing stands [39], [40], thus achieving the virtual cancellation of those perturbations. The compensation of harmonics of order 5, 7, 11, and 13 has been analyzed in this article, as they are responsible of the bulk of harmonic problems in this type of installations. Fig. 13 shows the evolution of the rms values of some of these harmonic currents during the first 100 s of the load profile taken as a benchmark in this article. Under these working conditions, Fig. 14 shows a snapshot of the voltage at the PCC, the output voltage of the STATCOM, and the corresponding currents.

In Fig. 14, the low distortion level of both the voltage at the PCC and the current flowing into the grid upstream from this point can be appreciated. Fig. 15 shows the corresponding spectra. Table IV confirms this perception offering numerical results derived from the analysis of the aforementioned signals.

Due to the inclusion of the STATCOM, the passive filtering stages will turn to be far from full load during normal operating conditions. However, in the event of disconnection of any of the filtering branches, the STATCOM automatically emulates the missing branch, including both its share in reactive power

TABLE IV
INDIVIDUAL DISTORTION INDEXES AND CURRENT THD*

	$I_{60\text{Hz}}$ (Arms)	$I_{300\text{Hz}}$ (%)	$I_{420\text{Hz}}$ (%)	$I_{660\text{Hz}}$ (%)	$I_{780\text{Hz}}$ (%)	THD (%)
STANDS	1082.0	3.40	1.80	2.00	1.00	4.55
STATCOM	151.4	3.27	1.90	2.10	1.10	32.37
GRID	638.2	0.29	0.13	0.02	0.04	0.76

*Calculated under 60 cycles with $t_{\text{initial}} = 25$ s; reference current = 1082 A.

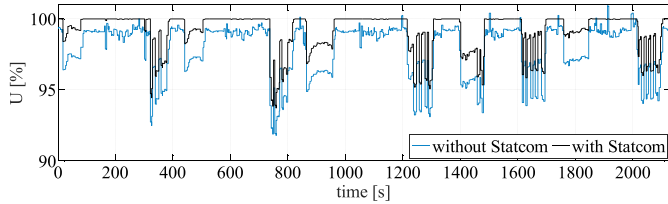


Fig. 16. Voltage drop at the PCC after the disconnection of the high pass band filter (12.5 Mvar). Effect of the support provided by the STATCOM.

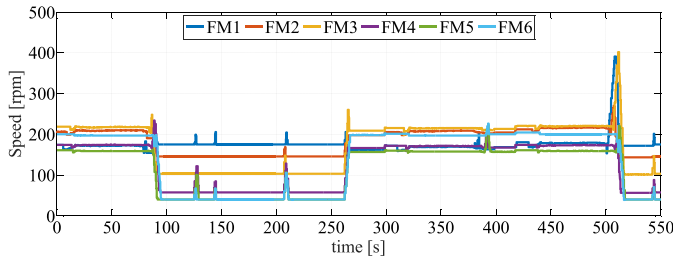


Fig. 17. Motor speed in the finishing mill stands.

compensation and its role in the cancellation of harmonics. The positive impact of the STATCOM in this situation can be observed in Fig. 16.

E. Objective 5: Inhibiting Resonances

The STATCOM is capable of inhibiting resonances that may be excited under certain rolling conditions. For this purpose, the controller of the device is endowed with sentinel current regulators qualified to absorb the impact of said resonances. The speed of the motors, which is depicted in Fig. 17, can be estimated from the rolling speed (Fig. 3) and the transmission ratios of the gearboxes. Focusing on the benchmark profile of Fig. 17, it is easy to check that the speed of the motor of the stand F3 is around 217.1 r/min between 0 and 80 s. As the said motor has three pole pairs, its supply frequency, f_0 is 10.86 Hz. For this specific operating frequency, a significant interharmonic arises at $f_1 + 12f_0 = 190.2$ Hz [20].

This frequency value lies near one of the resonant frequencies of the passive filtering system (Fig. 18) and could lead to an overcurrent condition both in the grid and in the filtering system. Under such damaging conditions, the STATCOM is able to inject a current component in the phase opposition of equal amplitude and frequency to the one demanded by the stands at the resonance frequency. A significant cancellation of the resulting current is achieved, thus effectively damping the resonant condition.

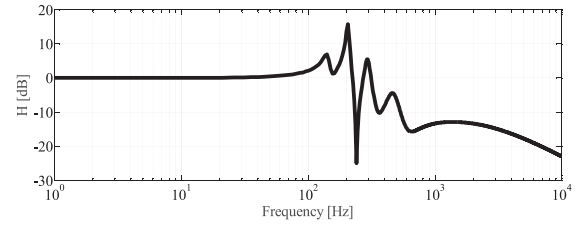


Fig. 18. Frequency response of the network with the parallel-connected filtering banks.

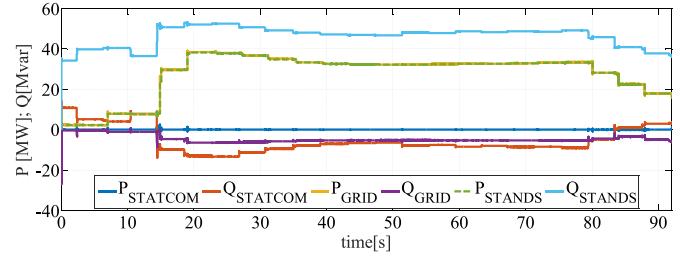


Fig. 19. Main active and reactive power flow between 0 and 95 s.

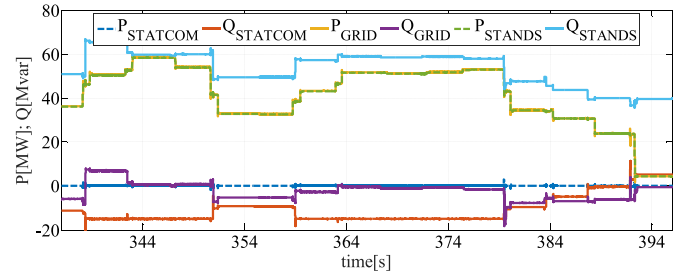


Fig. 20. Main active and reactive power flow between 336 and 400 s.

Resulting grid current is 16% of that corresponding to the resonant condition.

F. Joint Fulfillment of the Objectives

The behavior of the STATCOM while fulfilling simultaneously several of the targets described in the previous subsections is assessed. The transient response for reactive power flow different in sign and order of magnitude, as well as for diverse indexes of harmonic distortion is analyzed. Simulation results reproduce the behavior of the plant when subjected to the benchmark profile. Time references in the figures below are related to this profile.

Fig. 19 shows the evolution of the active and reactive power flows when the cylinders of the finishing mill are loaded and those of the roughing mill are not. Fig. 20 shows the evolution of the active and reactive power flows when two slabs overlap each other in the finishing and roughing mills.

Fig. 21 shows the evolution of the phase voltages and line currents under these conditions. Table V shows the main current distortion indexes. The resulting THD of the voltage at the PCC is 0.63%. Fig. 22 represents the evolution of the phase voltages and line currents; meanwhile, the rolling stands are not

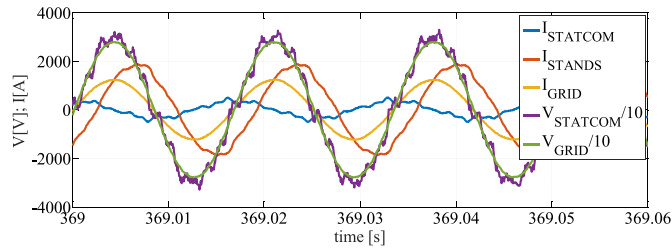


Fig. 21. Main variables: line currents and phase voltages.

TABLE V
INDIVIDUAL DISTORTION INDEXES AND CURRENT THD*

	$I_{60\text{Hz}}$ (Arms)	$I_{300\text{Hz}}$ (%)	$I_{420\text{Hz}}$ (%)	$I_{660\text{Hz}}$ (%)	$I_{780\text{Hz}}$ (%)	THD (%)
STANDS	1313.0	4.17	2.19	2.51	1.27	4.56
STATCOM	253.5	4.10	2.33	2.69	1.41	23.88
GRID	866.9	0.46	0.25	0.04	0.06	0.81

* Calculated under 60 cycles with $t_{\text{initial}} = 369$ s; reference current = 1082 A.

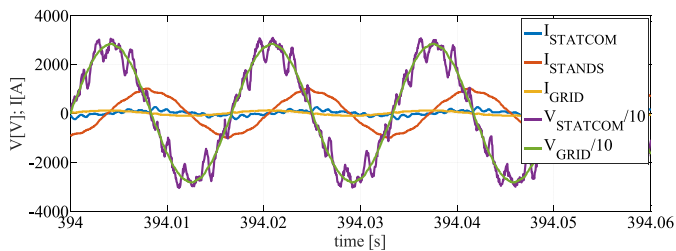


Fig. 22. Main variables: line currents and phase voltages.

loaded. In this case, the excess of reactive power provided by the passive filtering branch must be drawn from the system by the STATCOM.

VI. EXPERIMENTAL ANALYSIS

After concluding the full-scale design of the solution, as well as its validation through simulation, a small-scale experimental platform was developed. It was aimed to offer the technical managers of the rolling mill plant the opportunity to test, in real time and experimentally, the capabilities of the STATCOM under different rolling campaigns. The experimental platform can mimic the power flows of the real plant to scale. A small-scale prototype using two-level six-pulse converters was implemented and tested with the primary aim of emulating the following.

- 1) The demand for active and reactive power and the harmonic injection of the hot rolling mill plant, including the roughing mill, the finishing mill, and the passive filtering system. Thus, the operating conditions of the plant can be emulated, from an electrical point of view, before and after the incorporation of the STATCOM. The hot rolling mill plant is shown in Fig. 23 using a grey background.
- 2) The STATCOM response within the expected context. The scale STATCOM is capable of controlling the reactive power flow upstream of the PCC and thus of exerting a control action on the displacement factor and on the

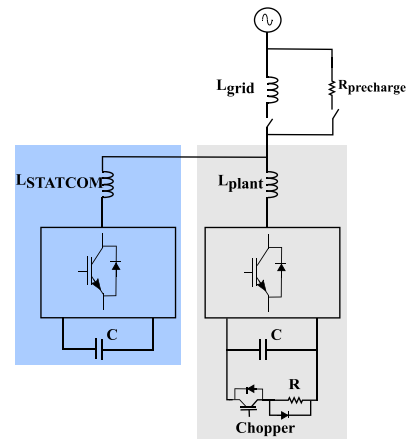
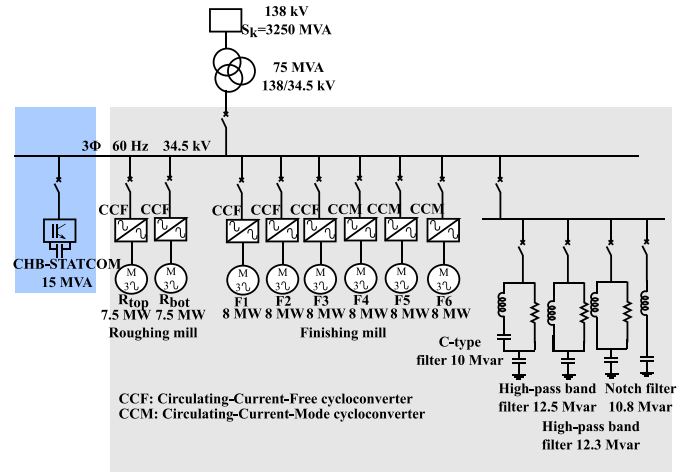


Fig. 23. Single-line diagram of the plant under analysis (top), and experimental platform used to emulate its operation (bottom).

TABLE VI
MAIN PARAMETERS OF THE EXPERIMENTAL SETUP

	PLANT	STATCOM
V_{grid} [V]	$120\sqrt{3}$	$120\sqrt{3}$
S_n [VA]	3000	750
f_c [kHz]	12.6	12.6
C [μF]	1100	1100

voltage at that point of coupling. This device is depicted in Fig. 23 on a blue background.

The scale plant is implemented by means of a converter. This converter uses an AFE rectifier with voltage-oriented control (VOC) which is commanded to maintain a constant DC bus voltage and to replicate the aggregated reactive power profile registered during the operation of the stands in the real plant. Furthermore, a resistive load is connected to the dc bus through a chopper, which is controlled to reproduce the aggregated active power profile of the plant. In this way, the dynamic behavior of the hot rolling mill can be accurately reproduced to scale (Fig. 23).

In order to replicate the behavior of the current harmonics injected by the stands, the values obtained during a measurement campaign are turned into active and reactive power fluctuations, which are added to the reactive and active power references of

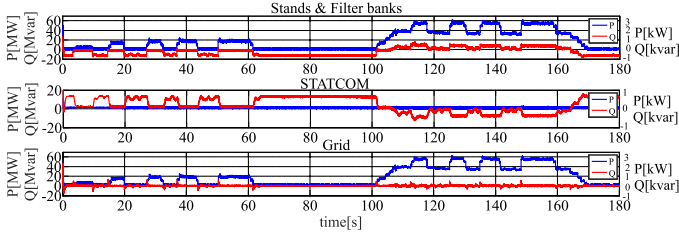


Fig. 24. Power profiles during the experimental tests. Two different scales are shown to account for the experimental test measurements and rescaled values.

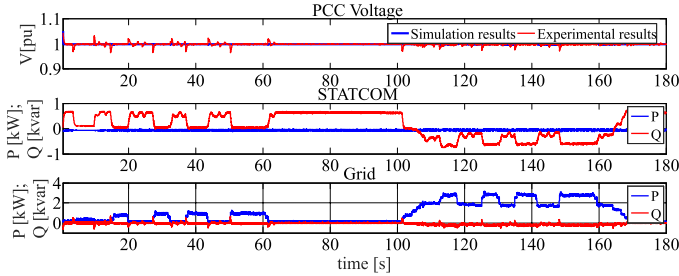


Fig. 25. Results obtained when the control of the PCC voltage is prioritized.

the converter and chopper, respectively. Conversely, the effect of the passive filter banks is based on an impedance model. The transfer function between the voltage at the point of connection and the current allows including the effect of the passive filter in the power references of the converter and chopper [41], [42]. The scaled STATCOM uses a second two-level six-pulse converter with VOC to emulate the operation of this piece of equipment. The reactive power reference for this converter is set according to the corresponding demand of reactive power and harmonics of the plant.

Undeniable differences exist between the topology of the STATCOM used in the experimental analysis and the one considered in the design and simulation stages, which not only affects their rated voltages and power (scaled at 1:166 and 1:20 000 respectively) but also their compensation capabilities. However, the experimental platform presented in this contribution allows demonstrating, at scale, that the STATCOM is capable of playing a valuable role in the context of a rolling mill plant in terms of a significant reduction of residual reactive power flows, the limitation of voltage variations, and the improvement of the displacement factor. Specifically, there are not important differences between the control algorithms used to compensate for the reactive power at the fundamental frequency in both scenarios. The achievement of these three objectives is illustrated in Figs. 24–26.

Fig. 24 depicts the power profile of the plant, STATCOM, and grid obtained experimentally during the rolling of two consecutive slabs. The first 60 seconds correspond to the operation of the roughing mill on a first slab subjected to five passes. From 100 to 168 s, the first slab is going through the finishing mill, whereas a new slab is being rolled by the roughing mill. The said values were obtained by conducting experimental tests where the adjustment of the displacement factor to a value close to unity was prioritized over the control of the PCC voltage. The global

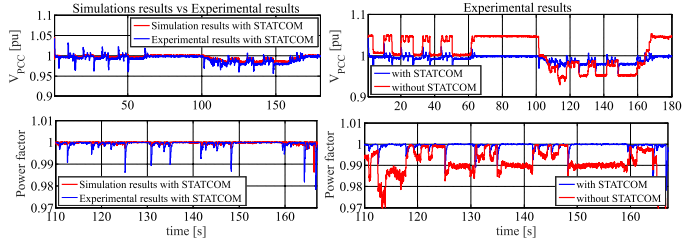


Fig. 26. Results obtained experimentally and under simulated actual conditions.

demand upstream the PCC is shown at the bottom of Fig. 24, where the cancellation of the reactive power flow through the network can be seen. The said cancellation is crucial to guarantee a displacement factor as close as possible to unity.

The PCC voltage and the power flow values when conducting an experimental test that prioritizes the control of the said voltage over the displacement factor correction are shown in Fig. 25. In this case, not only is the residual reactive power failed to be compensated for by the filtering system canceled, but a surplus of reactive energy is injected into the network in order to compensate for the voltage drop caused by the existing flow of active power. Fig. 26 shows simulation and experimental test results regarding the PCC voltage and the displacement factor upstream the PCC when one out of two alternate strategies prioritizing the control of either the former or the latter is adopted. The experimental results are clearly of the same order of magnitude as those obtained by simulating the observed differences being slight and due to conditions that are notably difficult to replicate.

Although the experimental platform reproduces the power flow at the fundamental frequency and its impact on the PCC voltage and the displacement factor accurately, the topology selected for the converter does not enable to properly assess the potential of the proposed control algorithm as for the management and control of harmonics injection since the frequency response of the said topology is significantly different from the actual one. Specifically, the results confirm a good match in the cancellation and control of reactive power flow at the fundamental frequency and on its impact on voltage regulation and PF. Notice that the analysis of all the implied variables can thus be carried out in real-time anticipating daily rolling mill campaigns of several hours. The use of simulation for such a task might be unfeasible or would require huge computational resources.

VII. CONCLUSION

Hot rolling mills are considered energy-intensive plants. At present, many of these installations use cycloconverter-based drives. A strategic use of a cascaded H-bridge based STATCOM can provide such type of plants with reactive power dynamic management, voltage control, and active mitigation of current harmonics. The solution proposed in this article is based on actual data of a real hot rolling mill and has been optimized through numerical simulations. Furthermore, an experimental validation of the solution is carried out at a laboratory scale. The article demonstrates that the use of this type of STATCOM

allows controlling the reactive power flows upstream from the PCC, exerting a rigorous control of the voltage at that point and reducing rapid voltage variations to comply with existing standards. Furthermore, the positive impact of this solution in the reduction of harmonic distortion is highlighted, together with its inherent capability to support the passive filtering system, avoiding unscheduled stops and damping inadvertent resonance conditions that may arise. Moreover, hot rolling mill plants are provided with the capacity for offering services linked to the management of reactive power and the improvement of power quality. Such services are of benefit to the internal operation of the plants and can be sold to the power system operator upstream the PCC.

REFERENCES

- [1] B. de Lamberterie, "Steel production - energy efficiency working group," ESTEP/EUROFER WG Energy Efficiency, European Commission, Final Rep., Jan. 2014.
- [2] C. S. Chen, Y. D. Lee, C. T. Hsu, D. S. Ting, and C. C. Shen, "Power quality assessment of a hot strip mill with cycloconverter drive systems," in *Proc. Ind. Appl. Conf. 42nd IAS Annu. Meeting*, New Orleans, LA, USA, 2007, pp. 9–16.
- [3] H. Hosoda, S. Kodama, and R. Tessenorf, "Large PWM inverters for rolling mills," *Assoc. Iron Steel Technol. Digit. Library*, Association for Iron & Steel Technology, USA, Jan. 2008.
- [4] J. R. Rodríguez *et al.*, "Technical evaluation and practical experience of high-power grinding mill drives in mining applications," *IEEE Trans. Ind. Appl.*, vol. 41, no. 3, pp. 866–874, May/Jun. 2005.
- [5] B. Chen and Y. Hsu, "An analytical approach to harmonic analysis and controller design of a STATCOM," *IEEE Trans. Power Del.*, vol. 22, no. 1, pp. 423–432, Jan. 2007.
- [6] M. Saeedifard, H. Nikkhajoei, and R. Iravani, "A space vector modulated STATCOM based on a three-level neutral point clamped converter," *IEEE Trans. Power Del.*, vol. 22, no. 2, pp. 1029–1039, Apr. 2007.
- [7] J. Lai and F. Z. Peng, "Multilevel converters—A new breed of power converters," *IEEE Trans. Ind. Appl.*, vol. 32, no. 3, pp. 509–517, May/Jun. 1996.
- [8] R. Xu *et al.*, "A novel control method for transformerless H-bridge cascaded STATCOM with star configuration," *IEEE Trans. Power Electron.*, vol. 30, no. 3, pp. 1189–1202, Mar. 2015.
- [9] J. Jung, J. Lee, S. Sul, G. Tae Son, and Y. Chung, "DC capacitor voltage balancing control for delta-connected cascaded H-bridge STATCOM considering unbalanced grid and load conditions," *IEEE Trans. Power Electron.*, vol. 33, no. 6, pp. 4726–4735, Jun. 2018.
- [10] A. S. Gadalla, X. Yan, S. Y. Altahir, and H. Hasabelrasul, "Evaluating the capacity of power and energy balance for cascaded H-bridge multilevel inverter using different PWM techniques," *J. Eng.*, vol. 2017, no. 13, pp. 1713–1718, 2017.
- [11] A. K. Chattopadhyay, "Alternating current drives in the steel industry, advancements in the last 30 years," *Ind. Electron. Mag.*, vol. 4, pp. 30–42, Dec. 2010.
- [12] H. Akagi, "Classification, terminology, and application of the modular multilevel cascade converter (MMCC)," *IEEE Trans. Power Electron.*, vol. 26, no. 11, pp. 3119–3130, Nov. 2011.
- [13] J. Rodriguez, S. Bernet, B. Wu, J. O. Pontt, and S. Kouro, "Multi-level voltage-source-converter topologies for industrial medium-voltage drives," *IEEE Trans. Ind. Electron.*, vol. 54, no. 6, pp. 2930–2945, Dec. 2007.
- [14] *AISI/SAE Standard (American Iron and Steel Institute / Society of Automotive Engineers)*, SAE J403 1010, 2014.
- [15] Associação Brasileira de Normas Técnicas, NBR 6655 LN280 ABNT, 2015.
- [16] ASTM Standard Specification for Steel, Sheet and Strip, Hot-Rolled, Carbon, Structural, High-Strength Low-Alloy, With Improved Formability, and Ultra-High Strength, A1011 SS36, 2017.
- [17] M. P. Groover, *Fundamentals of Modern Manufacturing. Materials, Processes and Systems*, 4th ed. New York, NY, USA: Wiley, 2010, pp. 395–403.
- [18] G. A. Orcajo *et al.*, "Dynamic estimation of electrical demand in hot rolling mills," *IEEE Trans. Ind. Appl.*, vol. 52, no. 3, pp. 2714–2723, May/Jun. 2016.
- [19] Badrzadeh, K. S. Smith, and R. C. Wilson, "Designing passive harmonic filters for an aluminum smelting plant," *IEEE Trans. Ind. Appl.*, vol. 47, no. 2, pp. 973–983, Mar./Apr. 2011.
- [20] G. A. Orcajo *et al.*, "Overcurrent protection response of a hot rolling mill filtering system: Analysis of the process conditions" *IEEE Trans. Ind. Appl.*, vol. 53, no. 3, pp. 2596–2607, May/Jun. 2017.
- [21] *IEEE Recommended Practices and Requirements for Harmonic Control in Electrical Power Systems*, IEEE Standard 519-2014, 2014.
- [22] *Electromagnetic Compatibility (EMC) - Part 3-7: Limits - Assessment of Emission Limits for the Connection of Fluctuating Installations to MV, HV and EHV Power Systems*, IEC TR 61000-3-7, 2008.
- [23] *IEEE Guide—Adoption of IEC/TR 61000-3-7:2008, Electromagnetic Compatibility (EMC)—Limits—Assessment of Emission Limits for the Connection of Fluctuating Installations to MV, HV and EHV Power Systems*, IEEE Standard 1453.1-2012, 2012.
- [24] MathWorks, The MathWorks—MATLAB and Simulink for Technical Computing, 2010. [Online]. Available: <http://www.mathworks.com>
- [25] P. K. Steimer, O. Apeldoorn, B. Odegard, S. Bernet, and T. Brucker, "Very high power IGCT PEBB technology," in *Proc. IEEE 36th Power Electron. Specialists Conf.*, Recife, Brazil, 2005, pp. 1–7.
- [26] H. Akagi, S. Inoue, and T. Yoshii, "Control and performance of a transformerless cascade PWM STATCOM with star configuration," *IEEE Trans. Ind. Appl.*, vol. 43, no. 4, pp. 1041–1049, Jul./Aug. 2007.
- [27] S. Debnath, J. Qin, B. Bahrani, and M. Saeedifard, "Operation, control and applications of the modular multilevel converter: A review," *IEEE Trans. Power Electron.*, vol. 30, no. 1, pp. 37–53, Jan. 2015.
- [28] N.-Y. Dai and M.-C. Wong, "Design considerations of coupling inductance for active power filters," in *Proc. 6th IEEE Conf. Ind. Electron. Appl.*, Univ. Macau, Beijing, China, 2011, pp. 1370–1375.
- [29] H. M. P. and M. T. Bina, "A transformerless medium-voltage STATCOM topology based on extended modular multilevel converters," *IEEE Trans. Power Electron.*, vol. 26, no. 5, pp. 1534–1545, May 2011.
- [30] S. Lechat Sanjuan, "Voltage oriented control of three-phase boost PWM converters," M.S. thesis, Dept. Electric Power Eng., Chalmers Univ. Technol., Gothenburg, Sweden, 2010.
- [31] M. Liserre, R. Teodorescu, and F. Blaabjerg, "Multiple harmonics control for three-phase grid converter systems with the use of PI-RES current controller in a rotating frame," *IEEE Trans. Power Electron.*, vol. 21, no. 3, pp. 836–841, May 2006.
- [32] R. Bojoi, L. R. Limongi, F. Profumo, D. Ruiu, and A. Tenconi, "Analysis of current controllers for active power filters using selective harmonic compensation," *IEEJ Trans. Elect. Electron. Eng.*, vol. 4, no. 2, Mar. 2009, pp. 139–157.
- [33] F. T. Ghetti, A. A. Ferreira, H. A. C. Braga, and P. G. Barbosa, "A study of shunt active power filter based on modular multilevel converter (MMC)," in *Proc. 10th IEEE/IAS Int. Conf. Ind. Appl.*, 2012, pp. 1–6.
- [34] M. Zygmanski, B. Grzesik, and J. Michalak, "Power conditioning system with cascaded H-bridge multilevel converter—DC-link voltage balancing method," in *Proc. 14th Eur. Conf. Power Electron. Appl.*, 2011, pp. 1–10.
- [35] G. Farivar, B. Hredzak, and V. G. Agelidis, "Decoupled control system for cascaded H-bridge multilevel converter based STATCOM," *IEEE Trans. Ind. Electron.*, vol. 63, no. 1, pp. 322–331, Jan. 2016.
- [36] S. Debnath, J. Qin, B. Bahrani, M. Saeedifard, and P. Barbosa, "Operation, control, and applications of the modular multilevel converter: A review," *IEEE Trans. Power Electron.*, vol. 30, no. 1, pp. 37–53, Jan. 2015.
- [37] J. B. Gil, T. G. San Román, J. J. A. Rios, and P. S. Martin, "Reactive power pricing: A conceptual framework for remuneration and charging procedures," *IEEE Trans. Power Syst.*, vol. 15, no. 2, pp. 483–489, May 2000.
- [38] P. Lipka, S. S. Oren, R. P. O'Neill, and A. Castillo, "Running a more complete market with the SLP-IV-ACOPF," *IEEE Trans. Power Syst.*, vol. 32, no. 2, pp. 1139–1148, Mar. 2017.
- [39] M. I. M. Montero, E. R. Cadaval, and F. B. Gonzalez, "Comparison of control strategies for shunt active power filters in three-phase four-wire systems," *IEEE Trans. Power Electron.*, vol. 22, no. 1, pp. 229–236, Jan. 2007.
- [40] O. Vodyakho and C. C. Mi, "Three-level inverter-based shunt active power filter in three-phase three-wire and four-wire systems," *IEEE Trans. Power Electron.*, vol. 24, no. 5, pp. 1350–1363, May 2009.
- [41] Pablo Ardura G., "Advanced reactive power compensation systems in hot strip mills," PhD dissertation, Dept. Elect. Eng., Univ. Oviedo, Aviles, Spain, 2017.
- [42] G. Alonso Orcajo *et al.*, "Power quality improvement in a hot rolling mill plan using a cascaded H-bridge STATCOM," in *Proc. IEEE Ind. Appl. Soc. Annu. Meeting*, Baltimore, Maryland, USA, 2019, pp. 1–9.



Gonzalo Arturo Alonso Orcajo (Member, IEEE) was born in Gijón, Spain, in 1965. He received the M.Sc. and Ph.D. degrees in electrical engineering from the University of Oviedo, Gijón, Spain, in 1990 and 1998, respectively.

In 1992, he joined the Department of Electrical Engineering, University of Oviedo, where he is currently an Associate Professor. His main research interests include power quality in industrial power systems. In recent years, he has focused on the detection and location of faults in distribution systems and on reactive power compensation systems.



Joaquín Francisco Pedrayes González was born in Gijón, Spain, in 1973. He received the M.Sc. and Ph.D. degrees in electrical engineering from the University of Oviedo, Gijón, Spain, in 2001 and 2007, respectively.

He is currently an Assistant Professor with the University of Oviedo.



Josué Rodríguez Díez was born in Pravia, Spain, in 1989. He received the M.Sc. degree in electrical engineering in 2014 from the University of Oviedo, Gijón, Spain, where he is currently working toward the Ph.D. degree in electrical engineering.

He is currently with ArcelorMittal Global R&D Basque Country Research Centre, Spain. He was a Research Fellow with the Department of Electrical Engineering, University of Oviedo. He has worked for two years with Department of Beams Radio Frequency Power Amplifiers, CERN, Switzerland. His

research interests include EAF, raw material, the field of reactive power compensation systems, and power quality.



Carlos H. Rojas was born in Caracas Venezuela. He received the M.Sc. degree in electrical engineering from Simón Bolívar University, Caracas, Venezuela, in 1994, and the Ph.D. degree from the University of Oviedo, Gijón, Spain, in 2001.

He is currently an Assistant Professor with the University of Oviedo. His main research interests include FEM modelling of electrical machines, predictive maintenance of electrical equipment, and power quality in industrial power systems.



José M. Cano (Member, IEEE) was born in Oviedo, Spain, in 1971. He received the M.Sc. and Ph.D. degrees in electrical engineering from the University of Oviedo, Gijón, Spain, in 1996 and 2000, respectively.

In 1996, he joined the Department of Electrical Engineering, University of Oviedo, where he is currently a Full Professor. During 2012 and 2014, he was a Visiting Associate Professor with the Department of Electrical and Computing Engineering, University of British Columbia, Canada. His main research interests include power quality solutions for industry,

power converters, power system state estimation, distributed generation, and smart grids.



Pablo Ardura G. was born in Luarca, Spain, in 1986. He received the M.Sc. and Ph.D. degrees in electrical engineering from the University of Oviedo, Gijón, Spain, in 2010 and 2017, respectively.

From 2010 to 2014 he was with the Department of Electrical Engineering, University of Oviedo. In 2015, he joined the ArcelorMittal Global R&D Center, Aviles, Spain, where he is currently a Research Engineer. His research interests include power quality, power converters, energy storage, and waste-heat recovery systems for the steelmaking industry.



Joaquín G. Norniella was born in Gijón, Spain, in 1980. He received the M.Sc. and Ph.D. degrees in electrical engineering from the University of Oviedo, Gijón, Spain, in 2005 and 2012, respectively.

He was a Research and Development Engineer with the Department of Electronic Engineering, University of Oviedo, for 20 months beginning in February, 2007. In 2008 he joined, the Department of Electrical Engineering, University of Oviedo, where he is currently a Lecturer. His main research interests include power quality solutions for industry and power converters.



Diego Cifrián R. was born in Oviedo, Spain, in 1987. He received the M.Sc. degree in electrical engineering from the University of Oviedo, Gijón, Spain, in 2010.

In 2014, he joined ArcelorMittal, where he is currently working as an R&D Engineer with Global R&D Center, Aviles, Spain. His main research interests include innovative solutions for the steelmaking industry, focused on electrical and combustion process improvement.